JCTC Journal of Chemical Theory and Computation

Article

pubs.acs.org/JCTC

A Valence Bond Description of the Prefulvene Extended Conical Intersection Seam of Benzene

Lluís Blancafort[†] and Michael A. Robb*[,‡]

[†]Institut de Química Computacional and Departament de Química, Universitat de Girona, Campus de Montilivi, E-17071 Girona, Spain

[‡]Department of Chemistry, Imperial College London, London SW7 2AZ, United Kingdom

Supporting Information

ABSTRACT: The permutational isomers of the prefulvene-like minimum energy conical intersection lie on an extended conical intersection seam, where they are connected by higher symmetry structures. Here, we present a VB analysis of the electronic states involved along this extended seam. The VB method produces a spin-exchange density (ie. a bonding pattern) that provides the basis to assign resonance structures to the states. The results show that in the high symmetry region of the seam, the character of the states is dominated by the positive and negative combination of the Kekulé structures, (A+B) and (A−B). The low energy parts of the seam, comprised of lower symmetry conical intersection structures, are stabilized by mixing with the Dewar resonance structures. This feature is responsible for the stability of the benzvalene-like conical intersections. The validity of the VB model is confirmed by calculating the branching space vectors at this level of theory, which are in good agreement with the CASSCF calculated vectors. The VB analysis has also allowed us to complete our picture of the global seam, since it has provided the clue to locate a conical intersection saddle point that interconverts two minima of the prefulvene conical intersection where the carbon bent out of the plane is inverted and rotated by 60°. This saddle point has a benzvalene-like geometry, in agreement with the VB picture.

INTRODUCTION

When benzene[1−5] is irradiated, it fluoresces. When the energy of the irradiating light is increased above a threshold, this fluorescence vanishes. The reason for this is the opening up of the radiationless decay channel associated with a so-called prefulvene conical intersection, where a bond between the C_1 and C_3 ring atoms was formed. This was one of the first excited state problems where theory (conical intersections) and experimental photophysics (radiationless decay) came together to give a unified picture. In recent years, there has been renewed interest in the photophysics of benzene from the experimental and theoretical side.[6−13]

While conical intersections have been known of since the 1930s,[14−16] Zimmerman,[17] Michl,[18] and Ruedenberg et al.[19] were among the first to suggest that internal conversion occurring at a conical intersection was the key feature to understanding certain photochemical mechanisms. Modern theoretical developments began to occur once the necessary theoretical methods,[20−26] were developed that enabled the location of minimum energy (points) conical intersections (MECIs). The location of many such MECIs at low-energy demonstrated that such features were an essential part of photochemistry. The historical development of the subject has been summarized elegantly by Michl in the preface of a collective volume on conical intersections.[27] A second volume on this subject has just been published.[28]

We now know that conical intersections are not isolated points through which a reaction path proceeds but form extended "seams".[29,30,31] In the original experiments on benzene, the radiationless decay was inhibited by an activation barrier, and experiments used energies that were just slightly above that reaction barrier. With modern laser experiments, one can begin to explore more of the conical intersection seam away from the minimum energy conical intersection point (MECI). In a previous paper,[32] we mapped out the conical intersection seam in some detail. The purpose of the present paper is to provide a model to understand the relationship between these points using a valence bond model.

The previous computational study[32] yielded several critical points with symmetries D_{2h}, C_{2h}, C_{2v}, and C_s (lowest energy point on the conical intersection seam). In that study, the main idea was that permutational isomers of the conical intersections of lower symmetry are connected by intersections of higher symmetry, with all structures forming an extended seam. In other words, one can go on the potential energy surface from one conical intersection to its permutational isomers through the high symmetry intersections, without leaving the seam. We now show that for each of these structures one can formulate analytical conditions,[33] from valence bond (VB) theory, (i) for the existence of the conical intersection, (ii) for the nature of the branching plane, and (iii) for the VB wave functions at the conical intersection. These theoretical constructions can then be compared with numerical computations. The resulting theoretical picture is consistent with the connectivity of the different structures and improves our understanding of the extended seam associated with the prefulvene conical

Special Issue: Berny Schlegel Festschrift

Received: July 21, 2012
Published: August 30, 2012

dx.doi.org/10.1021/ct300625u | J. Chem. Theory Comput. 2012, 8, 4922−4930

intersections of benzene. Related ideas have also been explored recently in polyenes.[34]

REVIEW OF VB THEORY

Many years ago, we presented the theory, based upon VB methods, to rationalize the geometries of conical intersections of hydrocarbons.[35] Over many years, we have been able to understand the structures of many conical intersections using such methods.[36,37] These ideas have also been explored by others.[38−44] A full analysis of the case of three electrons in three orbitals and four electrons in four orbitals has recently been given by Vanni et al.[33] However, the six-electron/six-orbital problem does not seem to have been analyzed in detail from this perspective. (However, benzene has been treated by spin-coupled VB theory.[45]) In fact, the conical intersection seam of benzene offers an ideal case to carry out this analysis because the wave function is dominated by 'covalent' configurations, and the 'ionic' ones which are not considered by the Rumer functions play no role. (The VB method has been shown to work well for low lying (non-Rydberg) potential surfaces and conical intersection structures of many aromatic hydrocarbons.[46,4748−50]) Thus, one of the objectives in this paper is to rationalize and understand the connectivity of the seams of intersection in benzene using VB methods. In three- and four-electron problems, there are only two possible valence bond couplings corresponding to ground and excited states. However, for the six-electron problem, for singlet states, there are the five valence bond couplings corresponding to the two Kekulé structures and three Dewar couplings (Figure 1). Of

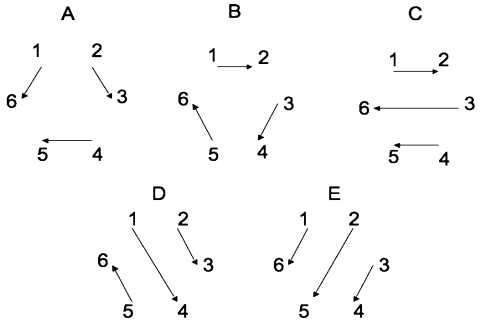

Figure 1. VB diagrams for six-electron systems.

course, the ground state is a combination of the two Kekulé structures; however, the nature of the first excited state has several possibilities which depend on the symmetry of the structure and which we will subsequently discuss.

We now give only the briefest possible theoretical presentation of a valence bond model and its application to the six orbitals of benzene. VB methods use a wave function which is a product of spin coupled pairs

$$\vartheta(s_i, s_j) = \frac{1}{\sqrt{2}}[\alpha(s_i)\beta(s_j) - \beta(s_i)\alpha(s_j)] \quad (1)$$

where the spin s_j is associated with a single orbital at position j. Each of these pairs is essentially a Heitler London VB wave function of the type familiar in the VB treatment of H_2. Thus, one of the Kekulé structures in benzene would be written as A = [23] [45] [16] (where [2,3] corresponds to $i = 2$, $j = 3$ in eq 1) and the other one would be B = [12] [34] [56]. Similarly, a Dewar structure would have the form C= [12] [45] [36]. These valence bond couplings are illustrated in Figure 1.

In terms of D_{6h} symmetry (see Table 1), A+B and C+D+E belong to A_{1g}. A−B belongs to B_{2u} while 2D−C−E and C−E

Table 1. Symmetry Descent for Benzene Rumer Functions

	D_{6h}	D_{2h}	C_{2v}	C_{2h}	C_s	C_2
A+B	A_{1g}	A_g	A_1	A_g	A'	A
A−B	B_{2u}	B_{3u}	B_1	A_u	A''	A
C−E	E_{1u}	B_{1u}	A_2	B_u	A''	B
2D−C−E	E_{1u}	A_u	A_1	A_g	A'	A
C+D+E	A_{1g}	A_g	A_1	A_g	A'	A

span E_{1u}. When the symmetry is lowered to the C_s subgroup (the σ plane in C_s corresponds to the $\sigma_v(14)$ in D_{6h}), the C−E basis function transforms as A'' and mixes with A−B. When the symmetry is lowered to C_2 (the out of plane C_2 axis in D_{6h}), both 2D−C−E and C−-E belong to the B irrep.

Full VB wave functions correspond to the eigenvectors obtained by diagonalization of the Hamiltonian in the space of these five basis functions. The matrix elements of the Hamiltonian are expressed in terms of exchange integrals between nonorthogonal orbitals and have the form $K_{ij} = [ij|ij] + S_{ij}h_{ij}$. The two-electron integral $[ij|ij]$ is assumed to be small and positive, while the integral h_{ij} is a nuclear−electron attraction integral which is negative and multiplied by the overlap S_{ij}. Thus, as expected, the exchange integrals are negative and depend upon the orbital overlap. These quantities can be fitted from *ab initio* data.[51] The indices i and j are associated with orbitals on nuclear centers i and j as in eq 1. The explicit formula for the matrix elements of this VB Hamiltonian is given in many places. A general treatment is given in the book by McWeeny and Sutcliffe.[52] All six electron matrix elements are given in Appendix 1. For example, the energy of a Kekulé structure is

$$H_{A,A} = Q + K_{16} + K_{23} + K_{45} - \frac{1}{2}(K_{12} + K_{34} + K_{56}) - \frac{1}{2}(K_{13} + K_{34} + K_{15} + K_{24} + K_{25} + K_{26} + K_{35} + K_{36} + K_{46}) \quad (2)$$

The symbol Q corresponds to the "coulomb energy," which would be the energy of the σ frame if all of the exchange integrals were identically zero. Q occurs in the energy of all five structures with the same numerical factor. Thus, for a given geometry this quantity provides the reference energy zero. The combination of the exchange integrals occurring in eq 2 is also easily understood. The positive terms K_{16}, K_{23}, and K_{45} correspond to the bonds (spin coupled pairs defined in eq 1) in structure A shown in Figure 1, while the negative terms occurring with the coefficient of −1/2 correspond to centers that are not directly bonded.

It is convenient to introduce the spin-coupling index P_{ij} for state I, which is just the coefficient of K_{ij} in eq 2, according to the formula

$$H_{I,I} = \sum_{ij} P_{ij}^I K_{ij} \quad (3)$$

For clarity, the superscript is ignored in the following. For a simple VB wave function, $P_{ij} = -1/2$ for uncoupled electron pairs and $P_{ij} = 1$ for spin coupled pairs. For instance, for structure A we have $P_{12} = -1/2$ and $P_{16} = 1$. Of course, in real VB functions (combinations of spin-coupled pairs), the

dx.doi.org/10.1021/ct300625u | J. Chem. Theory Comput. 2012, 8, 4922−4930

behavior is more complex. However, the point is that it is possible, using this index, to derive the VB function of the states involved at a conical intersection in a simple fashion. For our purposes, the P_{ij} index can be computed from a CASSCF wave function[53] or from a molecular mechanics valence bond (MMVB) wavefunction.[51]

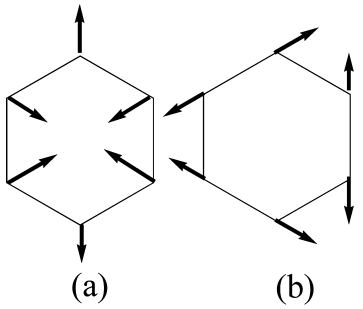

Figure 2. (a) Gradient difference $\nabla(H_{I,I} - H_{II,II})$ and (b) derivative coupling $\nabla H_{I,II}$ vectors for I = A+B and II = A−B, derived using the VB matrix elements (Appendix 1).

We now discuss how six-electron conical intersections can be studied in this VB formalism. The description of a given conical intersection can be specified by (i) a VB description of the two states (denoted I and II) involved in the conical intersection, (ii) a formula for the branching space vectors in terms of exchange integrals for (a) the energy difference between these states $(H_{I,I} - H_{II,II})$ and (b) the off−diagonal matrix element $H_{II,I}$. Note that neither of these quantities depend on Q (viz. eq 2). Thus, all our discussions about the conditions and branching space depend only on the exchange integrals.

These ideas are most easily understood using an example. Thus, let us consider the conical intersection between the superposition of two Kekulé structures I = A+B and the anti-Kekulé structure II = A−B.

Using the formulas in the Appendix, it is easily verified that

$$H_{I,I} - H_{II,II} = -K_{12} + 2K_{13} - K_{23} - 2K_{14} + 2K_{24} - K_{34} + 2K_{15} - 2K_{25} + 2K_{35} - K_{45} - K_{16} + 2K_{26} - 2K_{36} + 2K_{46} - K_{56} \quad (4a)$$

$$H_{I,II} = -K_{12} + K_{23} - K_{34} + K_{45} + K_{16} - K_{56} \quad (4b)$$

Note that $H_{II,I} \equiv 0$ for a molecule with a C_2 symmetry operation (corresponding to the permutation 2↔6 3↔5) and thus would be satisfied for D_{6h} benzene

At a conical intersection, we must have

$$(H_{I,I} - H_{II,II}) = 0 \text{ and } H_{I,II} = 0 \quad (5)$$

Further, we know[51] that K_{ij} has the form $K_{ij} \propto \exp(-bR_{ij})$ where R_{ij} is the distance between centers i and j. Thus, these formulas can either be used qualitatively, or if one knows the orientation between the orbitals i and j, the K_{ij} can be obtained in numerical form using the formulas that have been derived[51] from ab initio data.

The branching space of a conical intersection corresponds to vectors parallel to $\partial(H_{I,I} - H_{II,II})/\partial Q_i$ and $\partial H_{I,II}/\partial Q_i$ where Q_i are a set of internal coordinates. The magnitude of these gradients corresponds to $dK_{ij}/dR_{ij} \propto \exp(-bR_{ij})$ with direction along a unit vector from center i to center j. For this reason, we can use the direction of $(H_{I,I} - H_{II,II})$ and $\nabla(H_{I,I} - H_{II,II})$ interchangeably and similarly for $H_{I,II}$.

In Figure 2, we show these vectors for the Kekulé structure I = A+B and the anti-Kekulé structure II = A−B.

Now, we are in a position where we can state a general approach to the rationalization of computed points on the conical intersection seam for benzene. First, at any given critical point (i.e., given the geometry) we can postulate the nature of the VB states I and II. We can then test this hypothesis by evaluating the Hamiltonian numerically in terms of the exchange integrals using the formula given by Bernardi et al.[51] The P_{ij} can then be computed from the eigenvectors, and the resulting VB functions can be compared with the postulated ones. Given the values of the K_{ij}, we can obtain a numerical expression for $(H_{I,I} - H_{II,II}) = 0$ and $H_{I,II} = 0$ as a combination

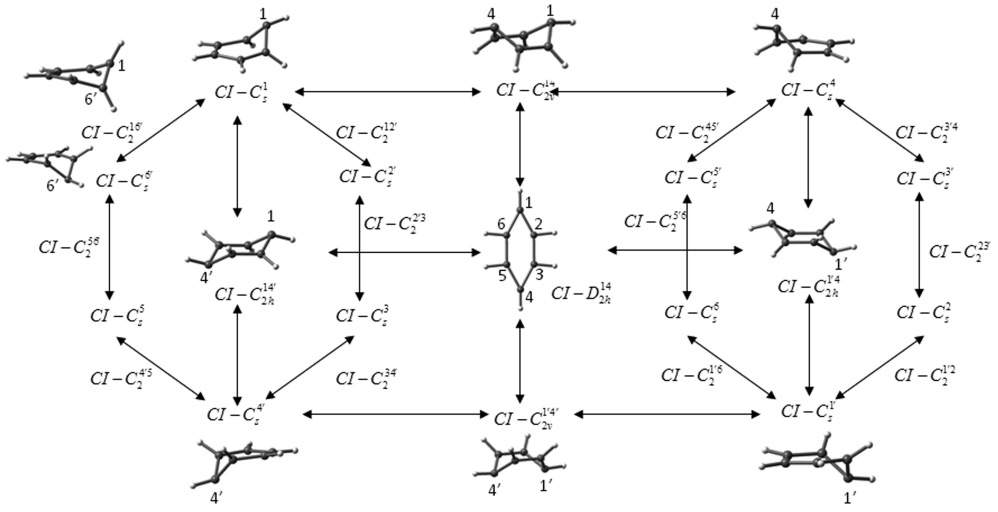

Figure 3. Connectivity scheme for the stationary points on the A/B conical intersection seam of benzene containing all permutational isomers of the prefulvene conical intersection (**CI-C_s**) with the same connectivity. The label superscripts refer to the carbon atoms that lie out of the plane; unprimed superscripts refer to atoms bent up with respect to the plane of the ring and primed ones to downward bent atoms. Some representative structures are included to illustrate the connectivity and the labeling.

of exchange integrals. This can be compared with analytical expressions obtained corresponding to various assumptions for I and II. One can also look at the problem from a different perspective. In the VB picture, any point on the conical intersection seam must satisfy a condition on the exchange integrals. This condition is only approximate, because unlike three electrons in three orbitals or four electrons in four orbitals there are five possible states involved rather than just two. However, understanding the relationship between the exchange integrals implied by $(H_{I,I} - H_{II,II}) = 0$ and $H_{I,II} = 0$ (for example eq 4a and 4b) still enables one to predict qualitatively the locus of points that may connect one MECI point and another.

In our previous mapping of the high-symmetry intersection space of benzene,[32] we found different seam branches that correlate with different states. The photochemically relevant one is the A/B branch, which correlates with the A′/A″ seam at the prefulvene intersection. This branch spans a series of conical intersections which are labeled according to their symmetry point group as **CI-D_{2h}**, **CI-C_{2v}**, **CI-C_{2h}**, **CI-C_s**, and **CI-C_2**. **CI-C_s** is the prefulvene conical intersection and the lowest-energy structure of the seam. The critical points on this seam are collected in Figure 3, where we illustrate the connectivity of the different permutational isomers through the high symmetry structures. In this paper, we will discuss this branch of the seam. The VB model just discussed, allows one to understand and explain why the points on the seam exist and how they can be connected.

COMPUTATIONAL DETAILS

The computational details for the location and characterization of the conical intersection critical points are given in ref 32. The optimizations are carried out at the CAS(6,6)/cc-pvdz level of theory, and the characterization of the critical points is done calculating the so-called intersection space frequencies.[23,30,54] The numerical VB calculations are carried out using the MMVB method.[51] All calculations are carried out using Gaussian Development Version[55]

RESULTS AND DISCUSSION

We will start with a discussion of the prefulvene **CI-C_s** intersection and then move upward in symmetry to consider the remaining intersections of the A/B seam branch. For comparison with the VB results, the branching space vectors computed at the CASSCF level are shown in Figure 4 for all critical points on the seam.

VB Analysis of the MECI Prefulvene-Like C_s Intersection. The prefulvene-like **CI-C_s** structure is the lowest MECI. We now derive analytical conditions for the conical intersection from VB and compare with numerical results obtained using the ab initio geometries and the exchange integral formulas from *ab initio* fitted data on model systems.[51] The prefulvene-like conical intersection structure is very close to an S_1 transition state that results from an avoided crossing of the anti-Kekulé state A−B and an antiquinoid structure (C−E) that has A″ symmetry in C_s. These states couple in this point group (Table 1) because they belong to the same irrep in C_s. Thus, as an example, we consider the conical intersection between *I* = A+B and II = A−B+C−E, where II is shown schematically in Figure 5. State II has a benzvalene-like, noncanonical VB structure. The remaining noncanonical VB structures are given in Appendix 2.

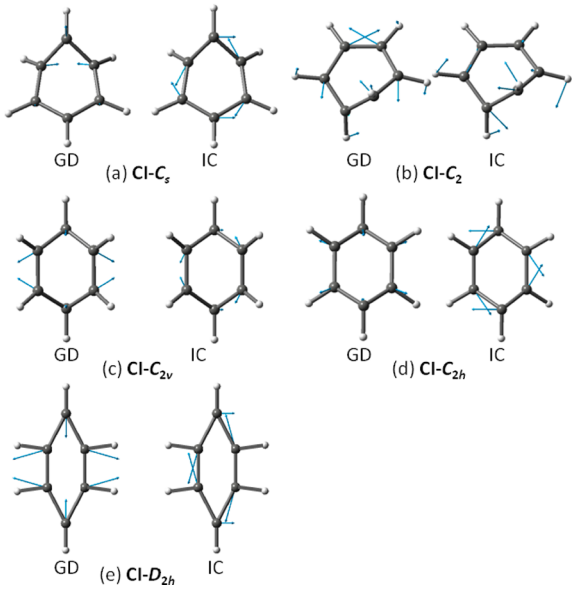

Figure 4. CASSCF branching space vectors at the conical intersections of the A/B branch of the benzene seam. GD = gradient difference vector; IC = interstate coupling.

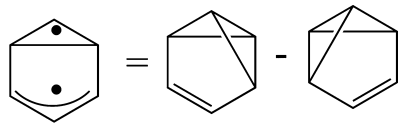

$$A+C \qquad B+E$$

$$=(A-B)+(C-E)$$

Figure 5. Prefulvene-like VB structure for state II at **CI-C_s**.

Let us first consider the spin-coupling indices P_{ij} for II, the prefulvene-like VB structure (see eq 3). The theoretical (in parentheses) and computed (MMVB) P_{ij} are contained in Table 2. The agreement is quite good, so we can confirm the nature of the VB structure given in Figure 5.

The energy difference and off diagonal matrix elements are given in eq 6:

$$H_{I,I} - H_{II,II} = 10K_{12} - 14K_{13} + 7K_{23} + 4K_{14} - 2K_{24} - 2K_{34} - 14K_{15} + K_{25} + 4K_{35} - 2K_{45} + 10K_{16} - 20K_{26} - K_{36} - 2K_{46} + 7K_{56} \quad (6a)$$

$$H_{I,II} = -18K_{12} + 6K_{13} + 12K_{23} - 6K_{24} - 6K_{34} - 6K_{15} + 12K_{25} + 6K_{45} + 18K_{16} + 12K_{36} + 6K_{46} - 12K_{56} \quad (6b)$$

Similar to what occurs for the intersection between the A+B and A−B states (eq 4b), one of the conditions for the conical intersection $H_{I,II} \equiv 0$ holds identically in the C_s point group, because of the reflection plane corresponding to the permutation 2 ↔ 6 and 3 ↔ 5. Equations 6a and 6b are illustrated schematically in Figure 6.

Notice the similarity to the numerical computed values in Figure 4a, and notice that the amplitude of motions of the

dx.doi.org/10.1021/ct300625u | J. Chem. Theory Comput. 2012, 8, 4922−4930

Table 2. Computed (MMVB) and Theoretical (in parentheses) P_{ij} Indices for the VB Structure of State II at CI-C_s (see Figure 5)

	i				
j	1	2	3	4	5
1					
2	−0.5 (−0.5)				
3	0.5 (0.5)	−0.4 (−0.5)			
4	−1.0 (−1.0)	−0.5 (−0.5)	0.5 (0.5)		
5	0.5 (0.5)	−0.7 (−1.0)	−0.9 (−1.0)	0.5 (0.5)	
6	−0.5 (−0.5)	0.9 (1.0)	−0.7 (−1.0)	−0.5 (−0.5)	−0.3 (−0.5)

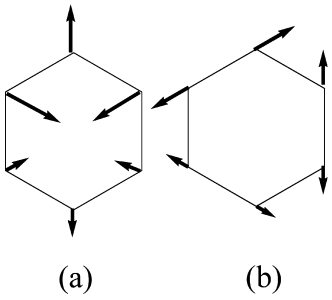

Figure 6. (a) Gradient difference $\nabla(H_{I,I} - H_{II,II})$ and (b) interstate coupling $\nabla H_{I,II}$ vectors for I = A+B and II = A−B+C−E, derived using the VB matrix elements (Appendix 1).

atoms 1−6−2 are enlarged while those of 3−4−5 are reduced compared to the (A+B)/(A−B) case (Figure 2a).

In Table 3, we give the computed coefficients of K_{ij} for $(H_{I,I} - H_{II,II})$ using the coefficients obtained from the ab initio

Table 3. Computed (MMVB) K_{ij} coefficients for $(H_{I,I} - H_{II,II})$ at the prefulvene intersection CI-C_s

	i				
j	1	2	3	4	5
1					
2	0.8				
3	−1.4	0.9			
4	1.2	−0.5	−0.2		
5	−1.4	0.4	0.2	−0.2	
6	0.8	−1.6	0.4	−0.5	0.9

geometry (reconverged using the exchange integrals computed using the formulas[51] fitted from ab intio model computations)

The ratios of the weights in Table 3 and the coefficients in eq 6a are in good agreement, especially for atoms 1−6−2. However, agreement can only be qualitative because we cannot know, a priori, the exact relative weights of A−B and C−E in state II (we have assumed equal weights for the analytical VB derivation).

Now we can summarize the preceding discussion of the MECI prefulvene CI structure, **CI-C_s**. We can start from a hypothesis that the intersecting states are the Kekulé state A+B and the combination of the anti-Kekulé state A−B and a combination of Dewar structures C−E. From this hypothesis, we can derive the spin coupling indices P_{ij} of the prefulvene state, II, and compare them with the numerical values (Table 2). Similarly, we can compare theoretical and numerical values for the characterization of the branching space (cf. Figure 4a vs Figure 6 and Table 3 vs eq 6a). We can conclude that the VB model yields a good framework for discussing the conical intersection seam in benzene. The VB picture can also be interpreted in terms of a *pseudo* Jahn−Teller effect between the B_{3u} and B_{1u} excited states at D_{2h} symmetry, which are B_1 and A_2 in C_{2v} (see Table 1). The lowest state (S_1) is the B_{3u} one. When the plane of symmetry perpendicular to $\sigma_v(14)$ is broken, both states become A″ and can mix. This is the origin of the energy lowering of the S_1 state that induces the intersection with the ground state.

Connection of Permutational Isomers of the Prefulvene CI-C_s. The question is now how to interconvert the conical intersection structures. We start by rotating the "prow" of **CI-C_s** by 60°, as shown in Figure 3 for ***CI*−C_s^1** and ***CI*−$C_s^{6'}$**. This can also be described as the interconversion of two adjacent isomers. The corresponding saddle point on the seam was not located in our previous work, but here we show how it can be predicted by the VB considerations. According to Figure 7, the VB wave function for state II of one isomer can be expressed as the sum (strictly speaking, the difference) of two benzvalene like structures, A+D and B+E. For the neighboring

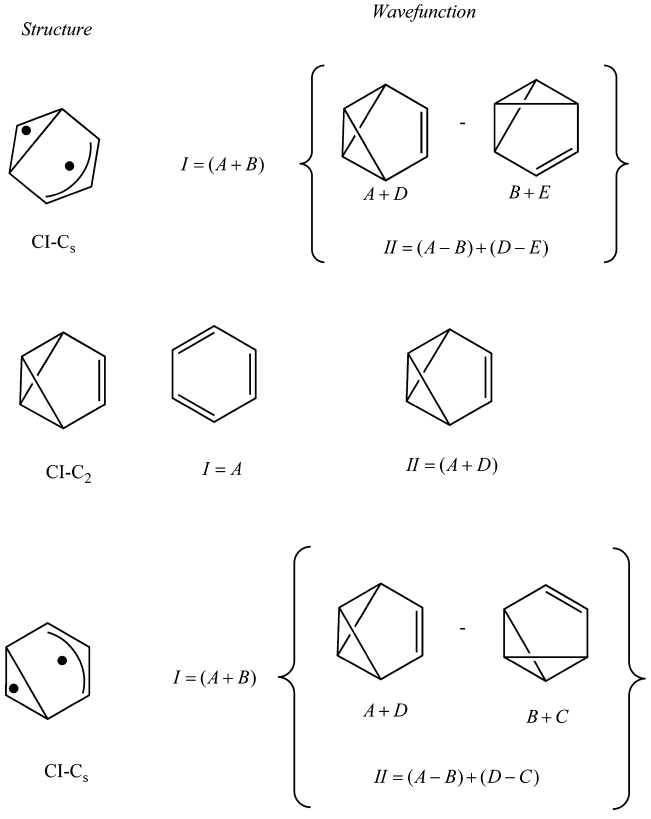

Figure 7. VB analysis for interconversion of two adjacent permutational isomers of **CI-C_s** prefulvene conical intersections through **CI-C_2**.

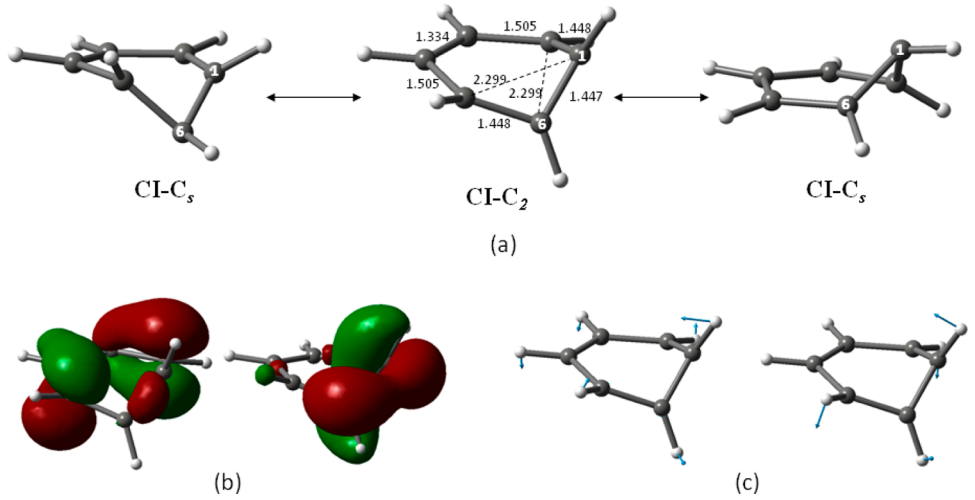

Figure 8. (a) Structure of **CI-C$_2$**, showing the interconversion of two **CI-C$_s$** permutational isomers (see also Figure 3). (b) Orbitals involved in the excitation. (c) Imaginary intersection space frequencies.

isomer, where the "prow" is rotated by 60°, the VB function is (A+D)−(B+C). This suggests that the VB function of state II for the intersection space saddle point that connects the two structures is A+D; i.e., the CI saddle point must have a benzvalene like geometry.

The CASSCF computations confirm such a conical intersection, **CI-C$_2$**. This structure belongs to the C_2 point group and lies 0.75 eV above the prefulvene **CI-C$_s$** intersection. The structure of **CI-C$_2$** is shown in Figure 8, together with the orbitals involved in the excitation. **CI-C$_2$** has two imaginary intersection space frequencies that interconvert two permutational isomers of **CI-C$_s$** (Figure 8c). **CI-C$_2$** not only rotates the prow by 60°, but it also inverts it with respect to the plane of the ring. This example, where a rather counterintuitive geometry is found, shows the heuristic value of the VB arguments.

Higher-Symmetry Conical Intersections. The situation for the interconversion of the 180° isomers is slightly more complicated. As we show in Figure 3, these isomers can be connected by an intersection of C_{2v} symmetry, **CI-C$_{2v}$**, where the two carbon atoms bent outward point in the same direction, or one of C_{2h} symmetry, **CI-C$_{2h}$**, where the 180° rotation occurs together with inversion of the '*prow*'. Both structures are described in our preceding study.[32] (In the Supporting Information, we also show a conical intersection of D_{3d} symmetry (at 4.2 eV above **CI-C$_s$**) not described in that study that connects three equivalent structures of **CI-C$_{2h}$**.) The VB analysis of the **CI-C$_{2h}$** and **CI-C$_{2v}$** intersections is given in Figure 9. Analysis of the computed P_{ij} for **CI-C$_{2v}$** clearly shows an intersection between A−B and a state dominated by D with a small admixture of A+B (i.e., $\delta < 1$ in Figure 9). The predominance of D is understandable because the antiquinoid structure is stabilized by the 1,4 interaction between the two carbon atoms that are bent out of the plane in the same direction. In contrast to this, the P_{ij} for **CI-C$_{2h}$** shows that the intersection involves only the Kekulé state A+B and the anti-Kekulé state A−B.

Finally, there is a highly compressed intersection of D_{2h} symmetry, **CI-D$_{2h}$**. To rationalize this intersection, we can return to our VB derivation of the GD (gradient difference) vector for the A+B and A−B states at D_{6h} symmetry (see eq 3a and Figure 2a). Figure 2a suggests that a conical intersection of

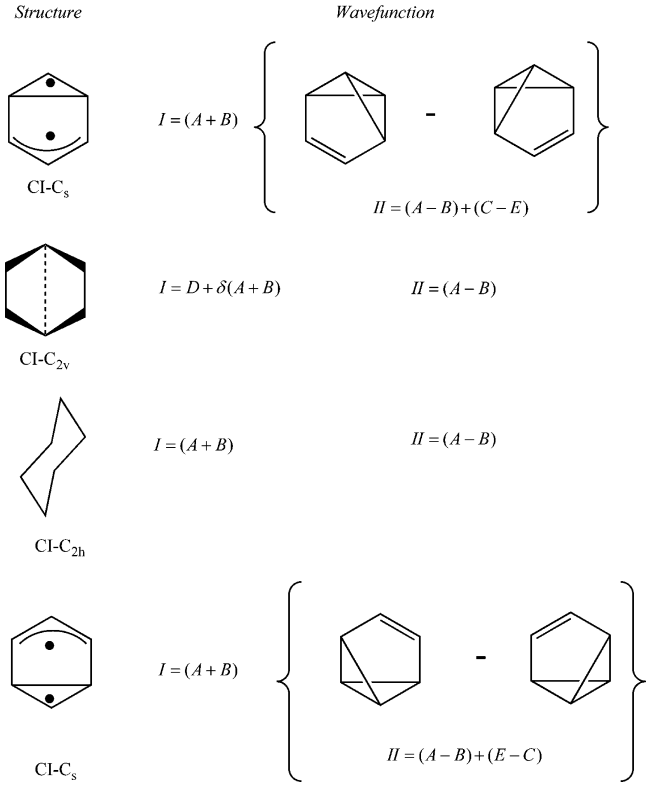

Figure 9. VB analysis for 180° interconversion of two permutational isomers of **CI-C$_s$** prefulvene conical intersection through **CI-C$_{2v}$** and **CI-C$_{2h}$**.

D_{2h} symmetry can be found along the GD vector, in agreement with the CASSCF computations.[32] The VB analysis also explains why no structure of D_{6h} symmetry exists on the A/B seam.

The computed CASSCF[53] P_{ij} indices in Figure 10 for **CI-D$_{2h}$** show that the VB structures have the form shown. In D_{2h} symmetry, the A+B state can mix with the C+D+E state (see Table 1), and the resulting wave function for state I can be described as A+B+C+D+E. The wave function for state II is given by A−B.

dx.doi.org/10.1021/ct300625u | J. Chem. Theory Comput. 2012, 8, 4922−4930

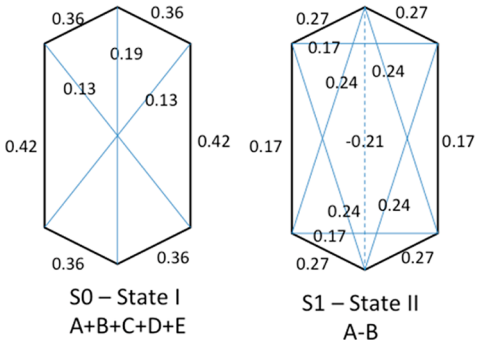

Figure 10. Computed CASSCF[53] P_{ij} indices for **CI-D_{2h}**.

CONCLUSIONS

VB ideas have proved[35] to be helpful to understand the structures of conical intersections, which often have high energy and have unusual geometries. In previous work, a VB analysis, of the type discussed in this paper has been applied to the three electrons in three orbitals problem or the four electrons in four orbitals one.[33] Such an analysis is slightly more complicated for benzene, since for this six electrons in six orbitals case there are five canonical valence bond structures. However, these structures are well-known, and the full set of matrix elements required to carry out the VB analysis is readily available. Therefore, in this paper we have extended the full VB analysis to benzene. The results have been compared with numerical *ab initio* computations, and the good agreement between the VB and *ab initio* models has confirmed the validity of the VB picture.

Because of its high symmetry, the conical intersection seam of benzene has a rich topology. There are 12 permutational isomers of the minimum energy, prefulvene-like conical intersection. In our preceding study, we showed that to understand the global topology it is essential to consider the high symmetry intersections that interconvert the different isomers. However, these structures are high in energy, and understanding the electronic structure factors that cause the degeneracy is difficult. The VB analysis presented in this paper provides such an understanding, since it has provided a VB based description, using resonance formulas, of the states at the different conical intersection stationary points. The high symmetry region of the seam is dominated by the positive and negative combinations of the Kekulé structures, (A+B) and (A−B), whereas the lower energy parts are stabilized by mixing the Dewar resonance structures. Moreover, the VB eigenfunctions can be classified according to the irreps of the symmetry point groups of the different structures. Therefore, the VB analysis can be completed with a rationalization of the changes in the wave function and the energy induced by mixing of the states as the symmetry is lowered, i.e., pseudo-Jahn−Teller effects. Apart from this 'a posteriori' rationalization of the conical intersections, the VB model has also suggested a new conical intersection saddle point that interconverts two prefulvene conical intersections through 60° rotation and inversion. The structure has C_2 symmetry and a benzvalene like geometry. This shows that the VB model is not only useful to rationalize available ab initio data but it can also be helpful in the search for new conical intersections.

APPENDIX 1

Six-in-six matrix elements

$$H_{AA} = Q + K_{16} + K_{23} + K_{45} - 1/2(K_{12} + K_{13} + K_{14} + K_{15} + K_{24} + K_{25} + K_{26} + K_{34} + K_{35} + K_{36} + K_{46} + K_{56})$$

$$H_{BB} = Q + K_{12} + K_{34} + K_{56} - 1/2(K_{16} + K_{13} + K_{14} + K_{15} + K_{24} + K_{25} + K_{26} + K_{23} + K_{35} + K_{36} + K_{46} + K_{45})$$

$$H_{CC} = Q + K_{12} + K_{36} + K_{45} - 1/2(K_{16} + K_{13} + K_{14} + K_{15} + K_{24} + K_{25} + K_{26} + K_{34} + K_{35} + K_{23} + K_{46} + K_{56})$$

$$H_{DD} = Q + K_{14} + K_{23} + K_{56} - 1/2(K_{12} + K_{13} + K_{16} + K_{15} + K_{24} + K_{25} + K_{26} + K_{34} + K_{35} + K_{36} + K_{46} + K_{45})$$

$$H_{EE} = Q + K_{16} + K_{25} + K_{34} - 1/2(K_{12} + K_{13} + K_{14} + K_{15} + K_{24} + K_{23} + K_{26} + K_{45} + K_{35} + K_{36} + K_{46} + K_{56})$$

$$H_{AB} = 1/4\{Q + K_{16} + K_{12} + K_{14} + K_{23} + K_{25} + K_{34} + K_{36} + K_{45} + K_{56} - 2(K_{13} + K_{15} + K_{24} + K_{26} + K_{35} + K_{46})\}$$

$$H_{AC} = 1/2\{Q + K_{16} + K_{12} + K_{23} + K_{36} + K_{45} - 2(K_{13} + K_{26}) - 1/2(K_{14} + K_{15} + K_{24} + K_{25} + K_{34} + K_{35} + K_{46} + K_{56})\}$$

$$H_{AD} = -1/2\{Q + K_{16} + K_{14} + K_{23} + K_{45} + K_{56} - 2(K_{15} + K_{46}) - 1/2(K_{12} + K_{13} + K_{24} + K_{25} + K_{26} + K_{34} + K_{35} + K_{36})\}$$

$$H_{AE} = -1/2\{Q + K_{16} + K_{25} + K_{23} + K_{34} + K_{45} - 2(K_{24} + K_{35}) - 1/2(K_{12} + K_{13} + K_{14} + K_{15} + K_{26} + K_{36} + K_{46} + K_{56})\}$$

$$H_{BC} = -1/2\{Q + K_{12} + K_{34} + K_{36} + K_{45} + K_{56} - 2(K_{35} + K_{46}) - 1/2(K_{13} + K_{14} + K_{15} + K_{16} + K_{23} + K_{24} + K_{25} + K_{26})\}$$

$$H_{BD} = -1/2\{Q + K_{12} + K_{14} + K_{23} + K_{34} + K_{56} - 2(K_{13} + K_{24}) - 1/2(K_{15} + K_{25} + K_{35} + K_{45} + K_{16} + K_{26} + K_{36} + K_{46})\}$$

$$H_{BE} = -1/2\{Q + K_{12} + K_{16} + K_{25} + K_{34} + K_{56} - 2(K_{15} + K_{26}) - 1/2(K_{13} + K_{23} + K_{35} + K_{36} + K_{14} + K_{24} + K_{45} + K_{46})\}$$

$$H_{CD} = 1/4\{Q + K_{12} + K_{14} + K_{16} + K_{23} + K_{25} + K_{34} + K_{36} + K_{45} + K_{56} - 2(K_{13} + K_{15} + K_{24} + K_{26} + K_{35} + K_{46})\}$$

$$H_{CE} = 1/4\{Q + K_{12} + K_{14} + K_{16} + K_{23} + K_{25} + K_{34} + K_{36} + K_{45} + K_{56} - 2(K_{13} + K_{15} + K_{24} + K_{26} + K_{35} + K_{46})\}$$

$$H_{DE} = 1/4\{Q + K_{12} + K_{14} + K_{16} + K_{23} + K_{25} + K_{34} + K_{36} + K_{45} + K_{56} - 2(K_{13} + K_{15} + K_{24} + K_{26} + K_{35} + K_{46})\}$$

APPENDIX 2

Benzvalene-like "crossed" VB diagrams for six-electron system

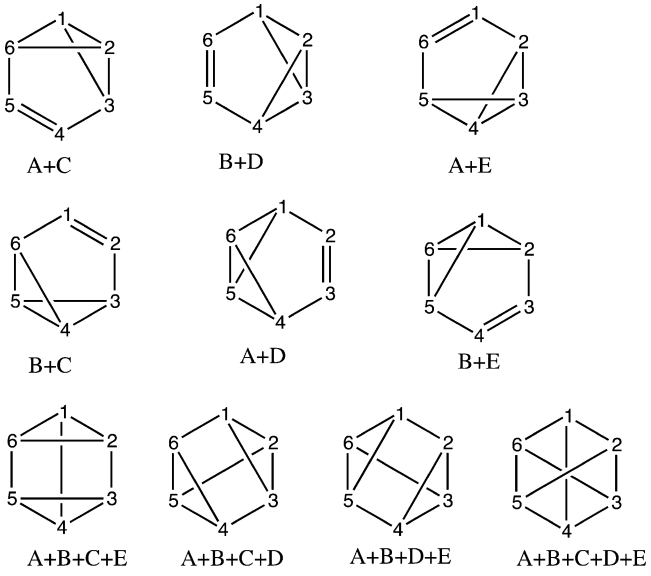

■ ASSOCIATED CONTENT

Supporting Information

Structure of **CI-D_{3d}**, including the branching space vectors, imaginary intersection space frequencies, and orbitals involved in the excitation. This material is available free of charge via the Internet at http://pubs.acs.org.

■ AUTHOR INFORMATION

Corresponding Author

*E-mail: mike.robb@imperial.ac.uk.

Notes

The authors declare no competing financial interest.

■ ACKNOWLEDGMENTS

We thank Q. Li for help with the CASSCF computations. This work has been supported by grants CTQ2011-26573 from the Spanish Ministerio de Economía y Competividad, SGR0528 from the Catalan Agència de Gestió d'Ajuts Universitaris i de Recerca (AGAUR), UNGI08-4E-003 from the Spanish Ministerio de Ciencia e Innovación and the FEDER fund (European Fund for Regional Development), and the Xarxa de Referència en Química Teòrica i Computacional de Catalunya from AGAUR. M.A.R. acknowledges a travel grant from AGAUR (2010PIV00086).

■ REFERENCES

(1) Bryce-Smith, D.; Gilbert, A. *Tetrahedron* **1976**, *32*, 1309.
(2) Moss, D. B.; Parmenter, C. S. *J. Phys. Chem.* **1986**, *90*, 1011.
(3) Longfellow, R. J.; Moss, D. B.; Parmenter, C. S. *J. Phys. Chem.* **1988**, *92*, 5438.
(4) Sobolewski, A. L.; Woywod, C.; Domcke, W. *J. Chem. Phys.* **1993**, *98*, 5627.
(5) Palmer, I. J.; Ragazos, I. N.; Bernardi, F.; Olivucci, M.; Robb, M. A. *J. Am. Chem. Soc.* **1993**, *115*, 673.
(6) Toniolo, A.; Thompson, A. L.; Martinez, T. J. *Chem. Phys.* **2004**, *304*, 133.
(7) Worth, G. A.J. *Photochem. Photobiol., A* **2007**, *190*, 190.
(8) Worth, G. A.; Carley, R. E.; Fielding, H. H. *Chem. Phys.* **2007**, *338*, 220.
(9) Parker, D. S. N.; Minns, R. S.; Penfold, T. J.; Worth, G. A.; Fielding, H. H. *Chem. Phys. Lett.* **2009**, *469*, 43.
(10) Penfold, T. J.; Worth, G. A. *J. Chem. Phys.* **2009**, *131*, 064303.
(11) Lasorne, B.; Bearpark, M. J.; Robb, M. A.; Worth, G. A. *J. Phys. Chem. A* **2008**, *112*, 13017.
(12) Minns, R. S.; Parker, D. S. N.; Penfold, T. J.; Worth, G. A.; Fielding, H. H. *Phys. Chem. Chem. Phys.* **2010**, *12*, 15607.
(13) Thompson, A. L.; Martinez, T. J. *Faraday Discuss.* **2011**, *150*, 293.
(14) von Neumann, J. W. *Phys. Z* **1929**, *30*, 467.
(15) Zerner, C. *Proc. R. Soc. A* **1932**, *137* (833, 696.
(16) Teller, E. *J. Phys. Chem.* **1937**, *41*, 109.
(17) Zimmerman, H. E. *J. Am. Chem. Soc.* **1966**, *88*, 2.
(18) Michl, J. *Mol. Photochem.* **1972**, 4.
(19) Atchity, G.; Xantheas, S.; Ruedenberg, K. *J. Chem. Phys.* **1991**, *95*, 1862.
(20) Ragazos, I.; Robb, M.; Bernardi, F.; Olivucci, M. *Chem. Phys. Lett.* **1992**, *197*, 217.
(21) Bearpark, M.; Robb, M.; Schlegel, H. *Chem. Phys. Lett.* **1994**, *223*, 269.
(22) Izzo, R.; Klessinger, M. *J. Comput. Chem.* **2000**, *21*, 52.
(23) Sicilia, F.; Blancafort, L.; Bearpark, M. J.; Robb, M. A. *J. Chem. Theory Comput.* **2008**, *4*, 257.
(24) Levine, B. G.; Coe, J. D.; Martinez, T. J. *J. Phys. Chem. B* **2008**, *112*, 405.
(25) Keal, T. W.; Koslowski, A.; Thiel, W. *Theor. Chem. Acc.* **2007**, *118*, 837.
(26) Maeda, S.; Ohno, K.; Morokuma, K. *J. Chem. Theory Comput.* **2010**, *6*, 1538.
(27) Domcke, W.; Yarkony, D. R.; Koppel, H. *Conical Intersections: Electronic Structure, Dynamics and Spectroscopy*; World Sci.: Singapore, 2004.
(28) Domcke, W.; Yarkony, D. R.; Koppel, H. *Conical Intersections: Theory, Computation and Experiment*; World Sci.: Singapore, 2011.
(29) Migani, A.; Robb, M.; Olivucci, M. *J. Am. Chem. Soc.* **2003**, *125*, 2804.
(30) Sicilia, F.; Blancafort, L.; Bearpark, M. J.; Robb, M. A. *J. Phys. Chem. A* **2007**, *111*, 2182.
(31) Robb, M. A. In *Conical Intersections, Theory, Computation and Experiment*; Domcke, W., Yarkony, D. R., Kopple, H., Eds.; World Sci.: Singapore, 2011; pp 3−50.
(32) Li, Q. S.; Mendive-Tapia, D.; Paterson, M. J.; Migani, A.; Bearpark, M. J.; Robb, M. A.; Blancafort, L. *Chem. Phys.* **2010**, *377*, 60.
(33) Vanni, S.; Garavelli, M.; Robb, M. A. *Chem. Phys.* **2008**, *347*, 46.
(34) Nenov, A.; de Vivie-Riedle, R. *J. Chem. Phys.* **2011**, 135.
(35) Bernardi, F.; Olivucci, M.; Robb, M.; Tonachini, G. *J. Am. Chem. Soc.* **1992**, *114*, 5805.
(36) Robb, M.; Garavelli, M.; Olivucci, M.; Bernardi, F. *Rev. Comput. Chem.* **2000**, *15*, 87.
(37) Bernardi, F.; Olivucci, M.; Robb, M. A. *Chem. Soc. Rev.* **1996**, *25*, 321.
(38) Wu, W.; Danovich, D.; Shurki, A.; Shaik, S. *J. Phys. Chem. A* **2000**, *104*, 8744.
(39) Ruiz, D. S.; Cembran, A.; Garavelli, M.; Olivucci, M.; Fuss, W. *Photochem. Photobiol.* **2002**, *76*, 622.
(40) Zilberg, S.; Haas, Y. *J. Phys. Chem. A* **1999**, *103*, 2364.
(41) Haas, Y.; Zilberg, S. *Adv. Chem. Phys.* **2002**, *124*, 433.
(42) Shaik, S.; Hiberty, P. C. *A Chemist's Guide to Valence Bond Theory*; Wiley Interscience: New York, 2007.
(43) Olsen, S.; McKenzie, R. H. *J. Chem. Phys.* **2009**, 131.
(44) Olsen, S.; McKenzie, R. H. *J. Chem. Phys.* **2009**, 130.
(45) Dasilva, E. C.; Gerratt, J.; Cooper, D. L.; Raimondi, M. *J. Chem. Phys.* **1994**, *101*, 3866.
(46) Smith, B.; Bearpark, M.; Robb, M.; Bernardi, F.; Olivucci, M. *Chem. Phys. Lett.* **1995**, *242*, 27.
(47) Bearpark, M.; Bernardi, F.; Clifford, S.; Olivucci, M.; Robb, M.; Smith, B.; Vreven, T. *J. Am. Chem. Soc.* **1996**, *118*, 169.
(48) Bearpark, M.; Bernardi, F.; Olivucci, M.; Robb, M. *Int. J. Quantum Chem.* **1996**, *60*, 505.
(49) Bearpark, M. J.; Bernardi, F.; Olivucci, M.; Robb, M. A. *J. Phys. Chem. A* **1997**, *101*, 8395.
(50) Bearpark, M.; Bernardi, F.; Olivucci, M.; Robb, M.; Smith, B. *J. Am. Chem. Soc.* **1996**, *118*, 5254.

(51) Bernardi, F.; Olivucci, M.; Robb, M. *J. Am. Chem. Soc.* **1992**, *114*, 1606.
(52) McWeeny, R.; Sutcliffe, B. T. *Methods of molecular quantum mechanics*; Academic Press: London, England, 1965.
(53) Blancafort, L.; Celani, P.; Bearpark, M.; Robb, M. *Theor. Chem. Acc.* **2003**, *110*, 92.
(54) Lasorne, B.; Sicilia, F.; Bearpark, M. J.; Robb, M. A.; Worth, G. A.; Blancafort, L. *J. Chem. Phys.* **2008**, *128*, 124307.
(55) Frisch, M. J.; Trucks, G. W.; Schlegel, H. B.; Scuseria, G. E.; Robb, M. A.; Cheeseman, J. R.; Scalmani, G.; Barone, V.; Mennucci, B.; Petersson, G. A.; Nakatsuji, H.; Caricato, M.; Li, X.; Hratchian, H. P.; Izmaylov, A. F.; Bloino, J.; Zheng, G.; Sonnenberg, J. L.; Hada, M.; Ehara, M.; Toyota, K.; Fukuda, R.; Hasegawa, J.; Ishida, M.; Nakajima, T.; Honda, Y.; Kitao, O.; Nakai, H.; Vreven, T.; Montgomery, J. A., Jr.; Peralta, J. E.; Ogliaro, F.; Bearpark, M.; Heyd, J. J.; Brothers, E.; Kudin, K. N.; Staroverov, V. N.; Kobayashi, R.; Normand, J.; Raghavachari, K.; Rendell, A.; Burant, J. C.; Iyengar, S. S.; Tomasi, J.; Cossi, M.; Rega, N.; Millam, J. M.; Klene, M.; Knox, J. E.; Bakken, V.; Adamo, C.; Jaramillo, J.; Gomperts, R.; Stratmann, R. E.; Yazyev, O.; Austin, A. J.; Cammi, R.; Pomelli, C.; Ochterski, J. W.; Martin, R. L.; Morokuma, K.; Zakrzewski, V. G.; Voth, G.; Salvador, P.; Dannenberg, J. J.; Dapprich, S.; Parandekar, P. V.; Mayhall, N. J.; Daniels, A. D.; Farkas, O.; Foresman, J. B.; Ortiz, J. V.; Cioslowski, J.; Fox, D. J. *Gaussian Development Version*, Revision H.08; Gaussian, Inc.: Wallingford, CT, 2010.